

See discussions, stats, and author profiles for this publication at: <https://www.researchgate.net/publication/313858017>

Machine Learning Predicts Laboratory Earthquakes

Article · February 2017

DOI: 10.1002/2017gl074677

CITATIONS

22

READS

1,348

6 authors, including:



Bertrand Rouet-Leduc

Los Alamos National Laboratory

17 PUBLICATIONS 90 CITATIONS

[SEE PROFILE](#)



Colin Humphreys

Queen Mary, University of London

810 PUBLICATIONS 15,586 CITATIONS

[SEE PROFILE](#)

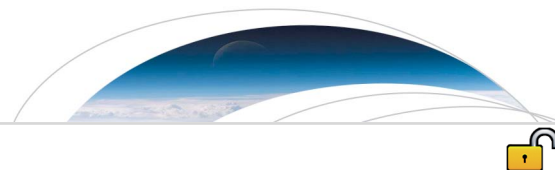
Some of the authors of this publication are also working on these related projects:



materials [View project](#)



Lighting the Future [View project](#)



RESEARCH LETTER

10.1002/2017GL074677

Key Points:

- Machine learning appears to discern the frictional state when applied to laboratory seismic data recorded during a shear experiment
- Machine learning uses statistical characteristics of the recorded seismic signal to accurately predict slip failure time
- We posit that similar machine learning approaches applied to geophysical data in Earth will provide insight in fault frictional processes

Supporting Information:

- Supporting Information S1

Correspondence to:

B. Rouet-Leduc,
bertrandr@lanl.gov

Citation:

Rouet-Leduc, B., Hulbert, C., Lubbers, N., Barros, K., Humphreys, C. J., & Johnson, P. A. (2017). Machine learning predicts laboratory earthquakes. *Geophysical Research Letters*, 44, 9276–9282. <https://doi.org/10.1002/2017GL074677>

Received 25 JUN 2017

Accepted 23 AUG 2017


Accepted article online 30 AUG 2017

Published online 22 SEP 2017

©2017. The Authors.

This is an open access article under the terms of the Creative Commons Attribution-NonCommercial-NoDerivs License, which permits use and distribution in any medium, provided the original work is properly cited, the use is non-commercial and no modifications or adaptations are made.

Machine Learning Predicts Laboratory Earthquakes

Bertrand Rouet-Leduc^{1,2}, Claudia Hulbert¹, Nicholas Lubbers^{1,3}, Kipton Barros¹, Colin J. Humphreys², and Paul A. Johnson⁴ 

¹Theoretical Division and CNLS, Los Alamos National Laboratory, Los Alamos, NM, USA, ²Department of Materials Science and Metallurgy, University of Cambridge, Cambridge, UK, ³Department of Physics, Boston University, Boston, MA, USA, ⁴Geophysics Group, Los Alamos National Laboratory, Los Alamos, NM, USA

Abstract We apply machine learning to data sets from shear laboratory experiments, with the goal of identifying hidden signals that precede earthquakes. Here we show that by listening to the acoustic signal emitted by a laboratory fault, machine learning can predict the time remaining before it fails with great accuracy. These predictions are based solely on the instantaneous physical characteristics of the acoustical signal and do not make use of its history. Surprisingly, machine learning identifies a signal emitted from the fault zone previously thought to be low-amplitude noise that enables failure forecasting throughout the laboratory quake cycle. We infer that this signal originates from continuous grain motions of the fault gouge as the fault blocks displace. We posit that applying this approach to continuous seismic data may lead to significant advances in identifying currently unknown signals, in providing new insights into fault physics, and in placing bounds on fault failure times.

Plain Language Summary Predicting the timing and magnitude of an earthquake is a fundamental goal of geoscientists. In a laboratory setting, we show we can predict “labquakes” by applying new developments in machine learning (ML), which exploits computer programs that expand and revise themselves based on new data. We use ML to identify telltale sounds—much like a squeaky door—that predict when a quake will occur. The experiment closely mimics Earth faulting, so the same approach may work in predicting timing, but not size, of an earthquake. This approach could be applied to predict avalanches, landslides, failure of machine parts, and more.

1. Introduction

A classical approach to determining that an earthquake may be looming is based on the interevent time (recurrence interval) for characteristic earthquakes, earthquakes that repeat periodically (Schwartz & Coppersmith, 1984). For instance, analysis of turbidite stratigraphy deposited during successive earthquakes dating back 10,000 years suggests that the Cascadia subduction zone is ripe for a megaquake (Goldfinger et al., 2017). The idea behind characteristic, repeating earthquakes was the basis of the well-known Parkfield prediction based strictly on seismic data. Similar earthquakes occurring between 1857 and 1966 suggested a recurrence interval of 21.9 ± 3.1 years, and thus, an earthquake was expected between 1988 and 1993 (Bakun & Lindh, 1985), but ultimately took place in 2004. With this approach, as earthquake recurrence is not constant for a given fault, event occurrence can only be inferred within large error bounds. Over the last 15 years, there has been renewed hope that progress can be made regarding forecasting owing to tremendous advances in instrumentation quality and density. These advances have led to exciting discoveries of previously unidentified slip processes that include slow slip (Melbourne & Webb, 2003), low frequency earthquakes and Earth tremor (Brown et al., 2009; Obara, 2002; Shelly et al., 2007) that occur deep in faults. These discoveries inform a new understanding of fault slip and may well lead to advances in forecasting, impending fault failure if the coupling of deep faults to the seismogenic zone can be unraveled. The advances in instrumentation sensitivity and density also provide new means to record small events that may be precursors. Acoustic/seismic precursors to failure appear to be a nearly universal phenomenon in materials. For instance, it is well established that failure in granular materials (Michlmayr et al., 2013) and in avalanche (Pradhan et al., 2006) is frequently accompanied by impulsive acoustic/seismic precursors, many of them very small. Precursors are also routinely observed in brittle failure of a spectrum of industrial (Huang et al., 1998) and Earth materials (Jaeger et al., 2007; Schubnel et al., 2013). Precursors are observed in laboratory faults (Goebel et al., 2013;

Johnson et al., 2013) and are widely but not systematically observed preceding earthquakes (Bouchon et al., 2013, 2016; Geller, 1997; McGuire et al., 2015; Mignan, 2014; Wyss & Booth, 1997). Seismic swarm activity which exhibits very different statistical characteristics than classical impulsive precursors may or may not precede large earthquakes but can mask classical precursors (e.g., Ishibashi, 1988). The International Commission on Earthquake Forecasting for Civil Protection concluded in 2011 that there was “considerable room for methodological improvements in this type of (precursor-based failure forecasting) research” (International Commission on Earthquake Forecasting for Civil Protection, 2011; Jordan et al., 2011). The commission also concluded that published results may be biased toward positive observations. We hypothesize that precursors are a manifestation of critical stress conditions preceding shear failure. We posit that seismic precursor magnitudes can be very small and thus frequently go unrecorded or unidentified. As instrumentation improves, precursors may ultimately be found to exist for most or all earthquakes (Delorey et al., 2017). Furthermore, it is plausible that other signals exist that presage failure.

2. Materials and Methods

Here we apply recent advances in machine learning to data from a well-characterized laboratory system (Johnson et al., 2013; Marone, 1998; Niemeijer et al., 2010; Scuderi et al., 2014). Our laboratory system is a two-fault configuration that contains fault gouge material submitted to double direct shear (see Text S1 and Figure S1 in the supporting information). The driving piston displaces at a very constant velocity of 5 $\mu\text{m/s}$ during the interevent time and accelerates briefly during slip with a calibrated accuracy of 0.1 $\mu\text{m/s}$. An accelerometer records the acoustic emission (AE) emanating from the shearing layers. The shear stress imposed by the driving block is also monitored (Figures 1, 2a, and S1), as well as other physical parameters such as the shearing rate, gouge layer thickness, friction, and the applied load (Johnson et al., 2013; Marone, 1998; Niemeijer et al., 2010). The steel blocks are extremely stiff (order 160 GPa), so the deformation takes place largely in the gouge. Following a stick-slip frictional failure (laboratory earthquake), the shearing block displaces while the gouge material simultaneously dilates and strengthens, as manifested by increasing shear stress (Figures 1a and S1) and friction. As the material approaches failure, it exhibits characteristics of a critical stress regime, including many small shear failures that emit impulsive AEs (Johnson et al., 2013). This unstable state concludes with a laboratory earthquake, in which the shearing block rapidly displaces, the friction and shear stress decrease precipitously due to the gouge failure (Figure S1, top), and the gouge layers simultaneously compact. Under a broad range of load and shear velocity conditions, the apparatus stick-slips quasi-periodically for hundreds of stress cycles during a single experiment (Marone, 1998; Niemeijer et al., 2010) and in general follows predictions from rate and state friction (e.g., Marone, 1998). The rate of impulsive precursors accelerates as failure approaches (Johnson et al., 2013), suggesting that upcoming laboratory earthquake timing could be predicted. In this work, we ask: Can the failure time of an upcoming laboratory earthquake be predicted using characteristics of only the continuously recorded acoustic signal?

Our goal is to predict the time remaining before the next failure (Figure 1a, bottom) using only local, moving time windows of the AE data (Figure 1b, top). We apply a machine learning technique, the random forest (RF) (Breiman, 2001; Louppe et al., 2013; Pedregosa et al., 2011), to the continuous acoustic time series data recorded from the fault (see Figure 1 and Texts S2 and S3). The RF model is an average over a set of decision trees (Figure 1c). Each decision tree predicts the time remaining before the next failure using a sequence of decisions based on statistical features derived from the time windows. Figure 1a (top) shows the laboratory shear stress exhibiting multiple failure events during an experiment.

From each time window, we compute a set of approximately 100 potentially relevant statistical features (e.g., mean, variance, kurtosis, and autocorrelation). The most useful features are then selected recursively (Gregorutti et al., 2017). The RF uses these selected features to predict the time remaining before the next failure (Text S4). Figure 1b shows four of these features on the same timescale as in Figure 1a, through multiple failure cycles. Some features are sensitive to changes in signal characteristics early in time during the stress cycle, just following a laboratory earthquake. All features shown are strongly sensitive to signal characteristics just preceding failure, as the system approaches shear-stress criticality.

3. Results

Figures 1d and 2 show failure predictions on testing data—the acoustic signal corresponding to a sequence of slip events that the model has never seen. We emphasize that there is no past or future information considered

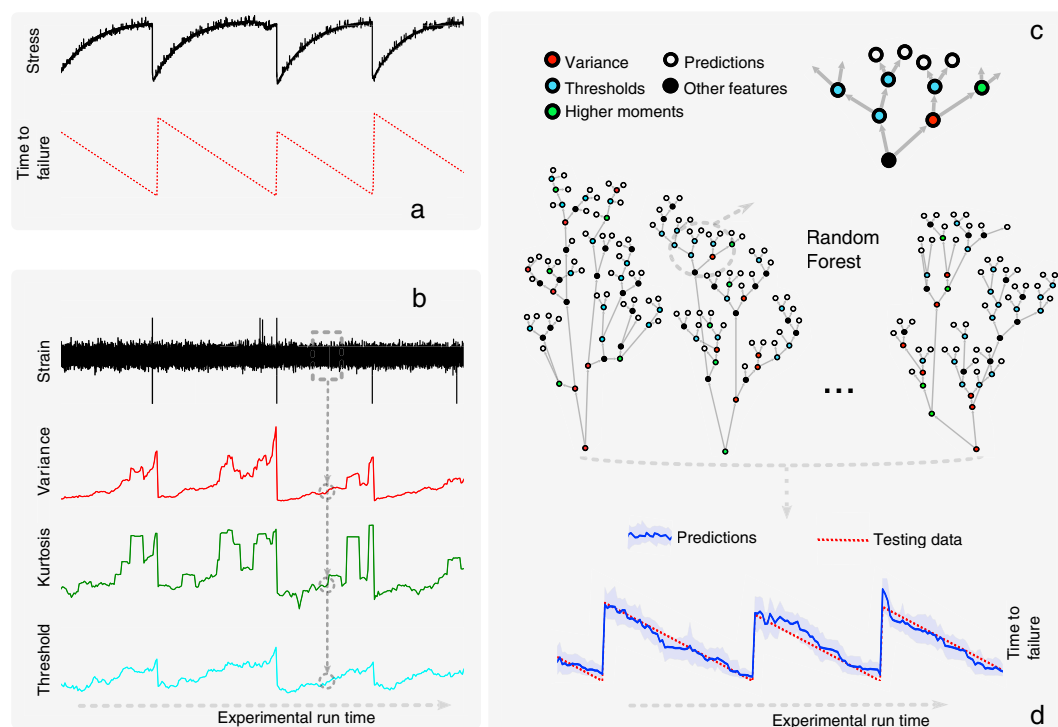


Figure 1. Random Forest (RF) approach for predicting time remaining before failure. (a) Shear stress (black curve) exhibits sharp drops, indicating failure events (laboratory earthquakes). We wish to predict the time remaining before the next failure derived from the shear stress drops (red curve), using only the (b) acoustic emission (dynamic strain) data. The dashed rectangle represents a moving time window; each window generates a single point on each feature curve below (e.g., variance and kurtosis). (c) The RF model predicts the time remaining before the next failure by averaging the predictions of 1,000 decision trees for each time window. Each tree makes its prediction (white leaf node), following a series of decisions (colored nodes) based on features of the acoustic signal during the current window (see supporting information S1). (d) The RF prediction (blue line) on data it has never seen (testing data) with 90% confidence intervals (blue shaded region). The predictions agree remarkably well with the actual remaining times before failure (red curve). We emphasize that the testing data are entirely independent of the training data, and were not used to construct the model. Data are from experiment number p2394.

when making a prediction (blue curve): each prediction uses only the information within one single time window of the acoustic signal. Thus, by listening to the acoustic signal currently emitted by the system, we predict the time remaining before it fails—a “now” prediction based on the instantaneous physical characteristics of the system that does not make use of its history. We quantify the accuracy of our model using R^2 , the coefficient of determination.

A naive model based exclusively on the periodicity of the events (average interevent time) only achieves an R^2 performance of 0.3 (see Figure S2). In comparison, the time to failure predictions from the RF model are highly accurate, with an R^2 value of 0.89. Surprisingly, the RF model accurately predicts failure not only when failure is imminent but also throughout the entire laboratory earthquake cycle, demonstrating that the system continuously progresses toward failure. This is unexpected, as impulsive precursors are only observed while the system is in a critical stress state. We find that statistics quantifying the signal amplitude distribution (e.g., its variance and higher-order moments) are highly effective at forecasting failure. The variance, which characterizes overall signal amplitude fluctuation, is the strongest single feature early in time (Figure 1b). As the system nears failure, other outlier statistics such as the kurtosis and thresholds become predictive as well. These outlier statistics are responding to the impulsive precursor AE (Figure 3c) typically observed as a material approaches failure (Huang et al., 1998), including those under shear conditions in the laboratory (Johnson et al., 2013) and in Earth (Bouchon et al., 2013, 2016; Wyss & Booth, 1997). These signals are due to small, observable shear failures within the gouge immediately preceding the laboratory earthquake (Johnson et al., 2013).

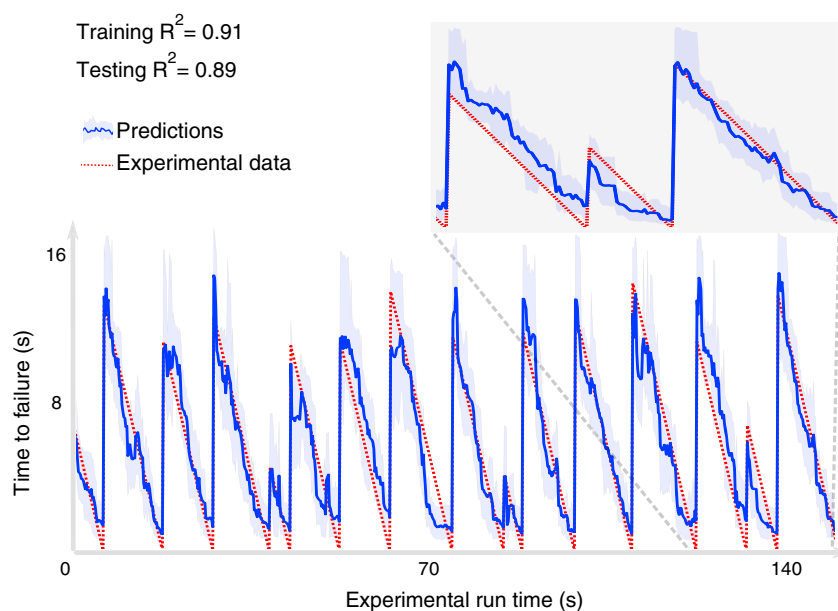


Figure 2. Time remaining before the next failure predicted by the Random Forest. As in Figure 1a, the red lines show the actual time before failure (Y axis) versus experimental run time (X axis). The red dashed line shows the time remaining before the next failure (derived from the shear stress data), and the blue line shows the corresponding prediction of the RF regression model (derived exclusively from the “instantaneous” acoustic data). The blue-shaded region indicates the 5th and 95th percentiles of the forecast; that is, 90% of the trees that comprise the forest made a forecast within these bounds. The inset emphasizes predictions on aperiodic slip behavior. The RF does a remarkable job of forecasting slip times even with aperiodic data. The RF was trained on ≈ 150 s of data (≈ 10 slip events), and tested on the following ≈ 150 s, shown here. We stress that the predictions from each time are entirely independent of past and future history—each blue point is a “now” prediction. The data points can be scrambled in time and the predictions remain the same. Data are from experiment number p2394.

Our machine learning analysis provides new insight into the slip physics. Specifically, the AE signal occurring long before failure was previously assumed to be noise and thus overlooked, illustrating human bias that ML can overcome (Johnson et al., 2013). This signal bears resemblance to nonvolcanic tremor (Brown et al., 2009; Obara, 2002; Shelly et al., 2007) associated with slow slip (Rogers & Dragert, 2003; Rubinstein et al., 2009), which exhibits ringing characteristics over long periods of time. An important difference is that tremor is isolated in time. In the laboratory experiments, the central block (Figure S1) slowly slips throughout the stress cycle, briefly accelerating at the time of failure. Figure (3b) shows a raw time series far from failure. The signal exhibits small modulations that are challenging to identify by eye and persist throughout the stress cycle. These modulations increase in amplitude as failure is approached, as measured by the increase in signal variance. This increase in signal variance shows that the energy carried by the acoustic signal steadily increases throughout the stress cycle. We posit that these variations are due to systematic groaning, creaking, and chattering from continuous grain motions of the fault gouge due to slow slipping of the block (Discrete Element Modeling of this system, Dorostkar et al. (2017a, 2017b) and Ferdowsi et al. (2014), is ongoing to further investigate the origin of this newfound signal). Our ML-driven analysis suggests that the system emits a small but progressively increasing amount of energy throughout the stress cycle, before abruptly releasing the accumulated energy when a slip event takes place (Figures S3 and S4). The predictions of our model generalize across experimental conditions. To demonstrate this, we trained the system at one applied load level and then tested it on data from different load levels, exhibiting different interevent times between failures. We observe that the model predictions retain their accuracy across load levels and correctly predicts clear outliers (see Figure S5). The fact that timing prediction can be made under conditions the RF has never seen suggests that the time series signal is capturing fundamental physics that leads to the prediction. Further, when the stress cycle periodicity is disrupted by a shorter recurrence time as shown in the inset of Figure 2, the RF still does an excellent job in predicting failure time, showing that the approach can be generalized to aperiodic fault cycles. Our physical interpretation is that the chattering signal variance and higher-order moments are a fingerprint of the instantaneous friction and shear stress state, the variance and other features of the time

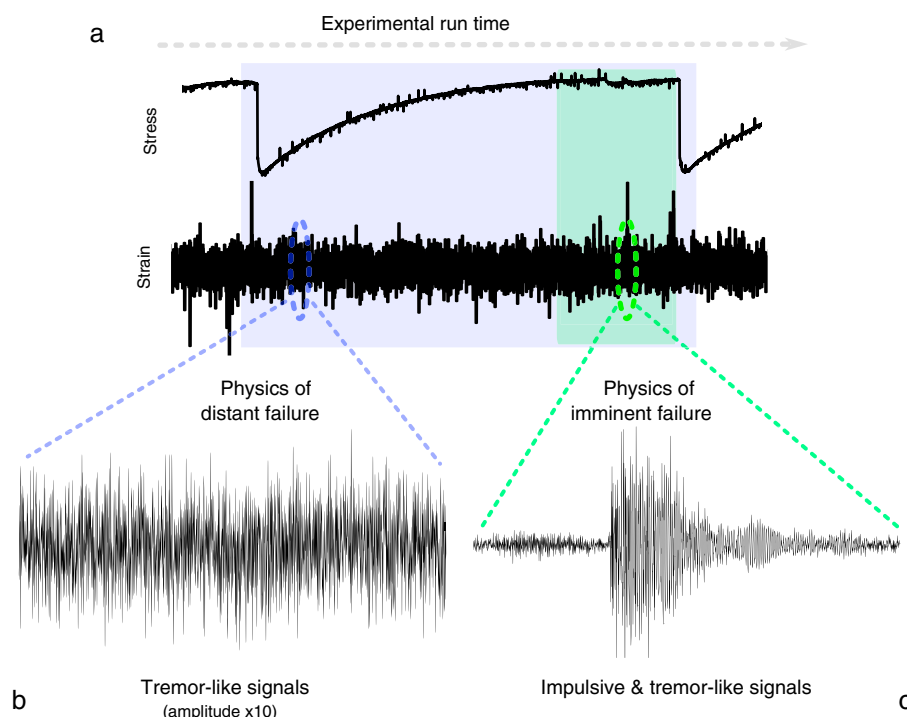


Figure 3. The physics of failure. The RF identifies two classes of signals and uses them to predict failure. (a) Shear stress and dynamic strain encompassing two failure events. (b) Zoom of dynamic strain when failure is in the distant future. This newly identified signal, termed “laboratory tremor” offers precise predictive capability of the next failure time. (c) Zoom of a classic, impulsive acoustic emission observed in the critically stressed region just preceding failure (note that vertical scale is different for two signals). Such signals are routinely identified preceding failure in the shear apparatus, in brittle failure in most materials and in some earthquakes. Data are from experiment number p2394.

series carry quantitative frictional state information (see Figures S3 and S4), informing the RF of when the next slip event will occur. If true, this is a remarkable observation in itself. We are currently working on the relation between the signal variance and friction to determine if indeed there is a direct link.

There are a number of issues to consider in applying what we have learned to Earth. The laboratory shear rates are orders of magnitude larger than Earth ($5 \mu\text{m/s}$ versus mms-cms/yr). The laboratory temperature conditions in no way resemble those in Earth, while the pressures could be representative of in situ pressures when fluid pressures are large. While it is a significant leap linking the laboratory studies to Earth scale, we know from past work (Goebel et al., 2013; Johnson et al., 2013) that the fundamental scaling relation in fault physics, the Gutenberg-Richter relation calculated from the laboratory precursors (Gutenberg & Richter, 1949), is within the bounds observed in Earth (Goebel et al., 2013; Johnson et al., 2013). This similarity implies that some of the important fault frictional physics scale. A laboratory experiment clearly cannot capture all of the physics of a complex rupture in Earth. Nevertheless, the machine learning expertise we are developing as we move from the laboratory to Earth will ultimately guide further work at large scale.

4. Conclusion

To summarize, we show that ML applied to this experiment provides accurate failure forecasts based on the instantaneous analysis of the acoustic signal at any time in the slip cycle and reveals a signal previously unidentified. These results should suffice to encourage ML analysis of seismic signals in Earth. To our knowledge, this is the first application of ML to continuous acoustic/seismic data with the goal of inferring failure times. These results suggest that previous analyses based exclusively on earthquake catalogs (Alves, 2006; Alexandridis et al., 2014; Keilis-Borok et al., 1988; Liu et al., 2005) may be incomplete. In particular, ML-based approaches mitigate human bias by automatically searching for patterns in a large space of potentially relevant variables. Our current approach is to progressively scale from the laboratory to the Earth by applying this approach to Earth problems that most resemble the laboratory system. An interesting analogy to the laboratory may be faults that exhibit small repeating earthquakes. For instance, fault patches located

on the San Andreas Fault near Parkfield (Nadeau & McEvilly, 1999; Zechar & Nadeau, 2012) exhibit such behavior. Repeaters at these fault patches may be emitting chattering in analogy to the laboratory. If so, can this signal be recorded by borehole and surface instruments? We are currently studying this problem. Whether ML approaches applied to continuous seismic or other geophysical data succeed in providing information on timing of earthquakes (not to mention the challenge of predicting earthquake magnitude), this approach may reveal unidentified signals associated with undiscovered fault physics. Furthermore, this method may be useful for failure prediction in a broad spectrum of industrial and natural materials. Technology is at a confluence of dramatic advances in instrumentation, machine learning, the ability to handle massive data sets and faster computers. Thus, the stage has been set for potentially marked advances in earthquake science.

Acknowledgments

We acknowledge funding from Institutional Support (LDRD) at Los Alamos National Laboratory including funding via the Center for Nonlinear Studies. We thank Chris Marone for access to and help with experiments, and comments to the manuscript. We thank Andrew Delorey, Thorne Lay, Christopher Ren, Barbara Romanowicz, Chris Scholz, and Bill Ellsworth for helpful comments and/or discussions. We thank Jamal Mohd-Yusof for suggesting applying machine learning to this data set. All the data used are freely available on the data repository hosted by Chris Marone at the Pennsylvania State University.

References

- Alexandridis, A., Chondrodima, E., Efthimiou, E., Papadakis, G., Vallianatos, F., & Triantis, D. (2014). Large earthquake occurrence estimation based on radial basis function neural networks. *IEEE Transactions on Geoscience and Remote Sensing*, 52(9), 5443–5453. <https://doi.org/10.1109/TGRS.2013.2288979>
- Alves, E. I. (2006). Earthquake forecasting using neural networks: Results and future work. *Nonlinear Dynamics*, 44(1), 341–349. <https://doi.org/10.1007/s11071-006-2018-1>
- Bakun, W. H., & Lindh, A. G. (1985). The Parkfield, California, earthquake prediction experiment. *Science*, 229, 619–624. <https://doi.org/10.1126/science.229.4714.619>
- Bouchon, M., Durand, V., Marsan, D., Karabulut, H., & Schmittbuhl, J. (2013). The long precursory phase of most large interplate earthquakes. *Nature Geoscience*, 6(4), 299–302.
- Bouchon, M., Marsan, D., Durand, V., Campillo, M., Perfettini, H., Madariaga, R., & Gardonio, B. (2016). Potential slab deformation and plunge prior to the Tohoku, Iquique and Maule earthquakes. *Nature Geoscience*, 9(5), 380–383.
- Breiman, L. (2001). Random forests. *Machine Learning*, 45(1), 5–32. <https://doi.org/10.1023/A:1010933404324>
- Brown, J. R., Beroza, G. C., Ide, S., Ohta, K., Shelly, D. R., Schwartz, S. Y., ... Kao, H. (2009). Deep low-frequency earthquakes in tremor localize to the plate interface in multiple subduction zones. *Geophysical Research Letters*, 36, L19306. <https://doi.org/10.1029/2009GL040027>
- Delorey, A. A., van der Elst, N. J., & Johnson, P. A. (2017). Tidal triggering of earthquakes suggests poroelastic behavior on the San Andreas Fault. *Earth and Planetary Science Letters*, 460, 164–170. <https://doi.org/10.1016/j.epsl.2016.12.014>
- Dorostkar, O., Guyer, R. A., Johnson, P. A., Marone, C., & Carmeliet, J. (2017a). On the micromechanics of slip events in sheared, fluid saturated fault gouge. *Geophysical Research Letters*, 44, 6101–6108. <https://doi.org/10.1002/2017GL073768>
- Dorostkar, O., Guyer, R. A., Johnson, P. A., Marone, C., & Carmeliet, J. (2017b). On the role of fluids in stick-slip dynamics of saturated granular fault gouge using a coupled computational fluid dynamics-discrete element approach. *Journal of Geophysical Research: Solid Earth*, 122, 3689–3700. <https://doi.org/10.1002/2017JB014099>
- Ferdowsi, B., Griffa, M., Guyer, R. A., Johnson, P. A., Marone, C., & Carmeliet, J. (2014). Three-dimensional discrete element modeling of triggered slip in sheared granular media. *Physical Review E*, 89, 42204. <https://doi.org/10.1103/PhysRevE.89.042204>
- Geller, R. J. (1997). Earthquake prediction: A critical review. *Geophysical Journal International*, 131(3), 425–450. <https://doi.org/10.1111/j.1365-246X.1997.tb06588.x>
- Goebel, T. H. W., Schorlemmer, D., Becker, T. W., Dresen, G., & Sammis, C. G. (2013). Acoustic emissions document stress changes over many seismic cycles in stick-slip experiments. *Geophysical Research Letters*, 40, 2049–2054. <https://doi.org/10.1002/grl.50507>
- Goldfinger, C., Galer, S., Beeson, J., Hamilton, T., Black, B., Romsos, C., Morey, A. (2017). The importance of site selection, sediment supply, and hydrodynamics: A case study of submarine paleoseismology on the Northern Cascadia margin, Washington, USA. *Marine Geology*, 384, 4–46. <https://doi.org/10.1016/j.margeo.2016.06.008>, subaquatic paleoseismology: records of large Holocene earthquakes in marine and lacustrine sediments.
- Gregorutti, B., Michel, B., & Saint-Pierre, P. (2017). Correlation and variable importance in random forests. *Statistics and Computing*, 27(3), 659–678.
- Gutenberg, B., & Richter, C. F. (1949). *Seismicity of the Earth*. Princeton, NJ: Princeton Univ. Press.
- Huang, M., Jiang, L., Liaw, P. K., Brooks, C. R., Seeley, R., & Klarstrom, D. L. (1998). Using acoustic emission in fatigue and fracture materials research. *Journal of Management*, 50(11), 1–14.
- International Commission on Earthquake Forecasting for Civil Protection (2011). Operational Earthquake Forecasting: State of Knowledge and Guidelines for Utilization. *Annals of Geophysics*, 54(4), 315–391. <https://doi.org/10.4401/ag-5350>
- Ishibashi, K. (1988). Two categories of earthquake precursors, physical and tectonic, and their roles in intermediate-term earthquake prediction. *Pure and Applied Geophysics*, 126(2), 687–700.
- Jaeger, J., Cook, N., & Zimmerman, R. (2007). Poroelasticity and Thermoelasticity. In *Fundamentals of Rock Mechanics* (pp. 168–204). Malden, MA: Blackwell.
- Johnson, P. A., Ferdowsi, B., Kaproth, B. M., Scuderi, M., Griffa, M., Carmeliet, J., ... Marone, C. (2013). Acoustic emission and microslip precursors to stick-slip failure in sheared granular material. *Geophysical Research Letters*, 40, 5627–5631. <https://doi.org/10.1002/2013GL057848>
- Jordan, T., Chen, Y.-T., Gasparini, P., Madariaga, R., Main, I., Marzocchi, W., ... Zschau, J. (2011). Operational earthquake forecasting. State of knowledge and guidelines for utilization. *Annals of Geophysics*, 54(4), 316–391. <https://doi.org/10.4401/ag-5350>
- Keilis-Borok, V., Knopoff, L., Rotwain, I., & Allen, C. (1988). Intermediate-term prediction of occurrence times of strong earthquakes. *Nature*, 335(6192), 690–694.
- Liu, Y., Li, Y., Li, G., Zhang, B., & Wu, G. (2005). Constructive ensemble of RBF neural networks and its application to earthquake prediction. *Advances in Neural Networks*, 3496, 532–537.
- Louppe, G., Wehenkel, L., Suter, A., & Geurts, P. (2013). Understanding variable importances in forests of randomized trees. In *Advances in Neural Information Processing Systems* (pp. 431–439).
- Marone, C. (1998). Laboratory-derived friction laws and their application to seismic faulting. *Annual Review of Earth and Planetary Sciences*, 26(1), 643–696.
- McGuire, J. J., Lohman, R. B., Catchings, R. D., Rymer, M. J., & Goldman, M. R. (2015). Relationships among seismic velocity, metamorphism, and seismic and aseismic fault slip in the Salton Sea Geothermal Field region. *Journal of Geophysical Research: Solid Earth*, 120, 2600–2615. <https://doi.org/10.1002/2014JB011579>

- Melbourne, T. I., & Webb, F. H. (2003). Slow but not quite silent, *Science*, 300(5627), 1886–1887. <http://dx.doi.org/10.1126/science.1086163>
- Michlmayr, G., Cohen, D., & Or, D. (2013). Shear-induced force fluctuations and acoustic emissions in granular material. *Journal of Geophysical Research: Solid Earth*, 118, 6086–6098. <https://doi.org/10.1002/2012JB009987>
- Mignan, A. (2014). The debate on the prognostic value of earthquake foreshocks: A meta-analysis. *Scientific Reports*, 4, 4099.
- Nadeau, R. M., & McEvilly, T. V. (1999). Fault slip rates at depth from recurrence intervals of repeating microearthquakes. *Science*, 285(5428), 718–721. <https://doi.org/10.1126/science.285.5428.718>
- Niemeijer, A., Marone, C., & Elsworth, D. (2010). Frictional strength and strain weakening in simulated fault gouge: Competition between geometrical weakening and chemical strengthening. *Journal of Geophysical Research*, 115, B10207. <https://doi.org/10.1029/2009JB000838>
- Obara, K. (2002). Nonvolcanic deep tremor associated with subduction in southwest Japan. *Science*, 296(5573), 1679–1681. <https://doi.org/10.1126/science.107037>
- Pedregosa, F., Varoquaux, G., Gramfort, A., Michel, V., Thirion, B., Grisel, O., ... Duchesnay, É. (2011). Scikit-learn: Machine learning in Python. *Journal of Machine Learning Research*, 12, 2825–2830.
- Pradhan, S., Hansen, A., & Hemmer, P. C. (2006). Crossover behavior in failure avalanches. *Physical Review E*, 74, 16122. <https://doi.org/10.1103/PhysRevE.74.016122>
- Rogers, G., & Dragert, H. (2003). Episodic tremor and slip on the Cascadia Subduction Zone: The chatter of silent slip. *Science*, 300(5627), 1942–1943. <https://doi.org/10.1126/science.1084783>
- Rubinstein, J. L., Shelly, D. R., & Ellsworth, W. L. (2009). Non-volcanic tremor: A window into the roots of fault zones. in *New Frontiers in Integrated Solid Earth Sciences* (pp. 287–314). New York: Springer.
- Schubnel, A., Brunet, F., Hilairet, N., Gasc, J., Wang, Y., & Green, H. W. (2013). Deep-focus earthquake analogs recorded at high pressure and temperature in the laboratory. *Science*, 341(6152), 1377–1380. <https://doi.org/10.1126/science.1240206>
- Schwartz, D. P., & Coppersmith, K. J. (1984). Fault behavior and characteristic earthquakes: Examples from the Wasatch and San Andreas Fault zones. *Journal of Geophysical Research*, 89(B7), 5681–5698. <https://doi.org/10.1029/JB089iB07p05681>
- Scuderi, M. M., Carpenter, B. M., & Marone, C. (2014). Physicochemical processes of frictional healing: Effects of water on stick-slip stress drop and friction of granular fault gouge. *Journal of Geophysical Research: Solid Earth*, 119, 4090–4105. <https://doi.org/10.1002/2013JB010641>
- Shelly, D. R., Beroza, G. C., & Ide, S. (2007). Non-volcanic tremor and low-frequency earthquake swarms. *Nature*, 446(7133), 305–307.
- Wyss, M., & Booth, D. C. (1997). The IASPEI procedure for the evaluation of earthquake precursors. *Geophysical Journal International*, 131(3), 423–424.
- Zechar, J. D., & Nadeau, R. M. (2012). Predictability of repeating earthquakes near Parkfield, California. *Geophysical Journal International*, 190(1), 457–462.